Raman spectroscopic study of (Pb1−xBax)(Yb1/2Ta1/2)O3 ceramics

Dibyaranjan Rout, V. Subramanian, K. Hariharan, V. R. Murthy, and V. Sivasubramanian

Citation: J. Appl. Phys. **98**, 103503 (2005); doi: 10.1063/1.2131188
View online: http://dx.doi.org/10.1063/1.2131188
View Table of Contents: http://jap.aip.org/resource/1/JAPIAU/v98/i10
Published by the AIP Publishing LLC.

Raman spectroscopic study of $(Pb_{1-x}Ba_x)(Yb_{1/2}Ta_{1/2})O_3$ ceramics

Dibyaranjan Rout, V. Subramanian,[a] K. Hariharan, and V. R. K. Murthy
Department of Physics, Indian Institute of Technology - Madras, Chennai-600 036, India

V. Sivasubramanian
Marerial Science Division, Indira Gandhi Center for Atomic Research, Kalpakkam- 603 102, India

(Received 10 March 2005; accepted 10 October 2005; published online 17 November 2005)

The ordered complex perovskite lead ytterbium tantalate undergoes a change in structural and dielectric properties as the concentration of Ba increases. The x-ray diffraction patterns show a decrease in the intensity of superlattice reflections due to Pb-antiparallel displacement as well as to *B*-site ordering. The structure approaches cubic symmetry with increase in Ba content. The dielectric response shows a gradual change from antiferroelectric to relaxor ferroelectric and then the relaxor behavior starts decreasing as Ba content increases. Raman-scattering study of the samples shows that some of the modes seen for $Pb(Yb_{0.5}Ta_{0.5})O_3$ disappear and an additional mode appears at 420 cm^{-1} with increase in Ba concentration. A qualitative analysis of various modes suggests that the substitution of Ba for Pb leads to a decrease in the degree of ordering and occurrence of local distortions in the lattice as evidenced by the broadening of certain peaks in the Raman spectra. © *2005 American Institute of Physics*. [DOI: 10.1063/1.2131188]

I. INTRODUCTION

Recently, a lot of attention has been given to the lead-based complex perovskites, specifically the compounds with chemical formula $Pb(B'_{1/2}B''_{1/2})O_3$ and their solid solutions, due to variety of physical properties and wide range of industrial applications.[1,2] Lead ytterbium tantalate $Pb(Yb_{0.5}Ta_{0.5})O_3$ (PYT) belongs to the group of lead-based complex perovskites which have long range *B*-site ordering. Room-temperature x-ray diffraction (XRD) pattern of PYT shows the presence of superlattice reflections due to *B*-site ordering and Pb-antiparallel displacement. Yasuda and Konda[3] have observed from the high-temperature XRD data that the crystal structure of PYT is cubic in paraelectric phase. The splitting of structure sensitive peaks in low-temperature (below T_c) XRD pattern can be interpreted as arising from orthorhombically distorted ABO_3-type subcells with the pseudomonoclinic cell parameters.[4–6] PYT undergoes two successive phase transitions: (i) a sharp first-order phase transition from paraelectric to antiferroelectric at 288 °C and (ii) a rather weak diffused phase transition from antiferroelectric to ferroelectric at 166 °C. The symmetries of the phases have not been clearly determined up to now and according to the suggestion made by Sciau *et al.*,[4] the cubic phase of PYT belongs to the space group $Fm\bar{3}m$ and the XRD patterns at 30 and 220 °C are both in agreement with the space group *Pbnm*. Our previous investigation on $(Pb_{1-x}Ba_x)(Yb_{0.5}Ta_{0.5})O_3$, $x=0.0$, 0.1, 0.15, 0.2, and 0.3, shows a significant enhancement of the dielectric properties with Ba concentration.[7] The temperature T_{max} corresponding to the maximum value of dielectric constant (ε_{max}) decreases with increase in Ba concentration. The dielectric constant increases and reaches a maximum value when $x=0.2$. At $x=0.2$, the compound exhibits diffuse phase transition with a small dielectric dispersion. Hence, a morphotropic phase boundary is inferred to exist around this composition range. The increase in diffuseness observed may be due to the decrease in *B*-site ordering as well as to the presence of polar clusters with local structure distortions within a nonpolar matrix. This can be partially evidenced by the decrease in the intensity of superlattice reflections in the x-ray diffraction data, when the concentration of Ba increases. Raman spectroscopy is a powerful light-scattering technique used to diagnose the internal structure of molecules and crystals.[8–10] It is also an appropriate technique to obtain information on the disorder and the strains in crystalline lattices, because vibrational spectroscopy has a shorter characteristic length scale than it is required for the diffraction experiment. For example, though the macroscopic crystal structure of $Pb(Mg_{1/3}Nb_{2/3})O_3$ is cubic, it exhibits a complex Raman spectrum and it has been interpreted as due to the existence of 1:1 *B*-site ordered nanoclusters and areas with local structural distortion, the symmetry of which is lower than cubic.[11,12] Setter and Laulicht and Bismayer *et al.*. have studied the Raman spectra of $Pb(Sc_{1/2}Ta_{1/2})O_3$ samples to observe the change in degree of ordering due to the effect of annealing and quenching processes.[9,13] As our system undergoes a change from antiferroelectric (ordered) to relaxor (disordered) and then tends towards dielectric (ordered) nature, it will be interesting to study the Raman spectra of the system to get more insight into the order-disorder and the local distortion present. The present paper reports on a detailed Raman spectroscopic study of $(Pb_{1-x}Ba_x)(Yb_{0.5}Ta_{0.5})O_3$, $x=0.0$, 0.1, 0.15, 0.2, 0.3, and 1.0, combined with x-ray diffraction analysis and dielectric constant measurements.

II. EXPERIMENTAL PROCEDURE

Polycrystalline samples of $(Pb_{1-x}Ba_x)(Yb_{0.5}Ta_{0.5})O_3$, $x=0.0$, 0.1, 0.15, 0.2, 0.3, and 1.0, were prepared by solid-

[a]Author to whom correspondence should be addressed; FAX: +91-044-22574852; electronic mail: manianvs@iitm.ac.in

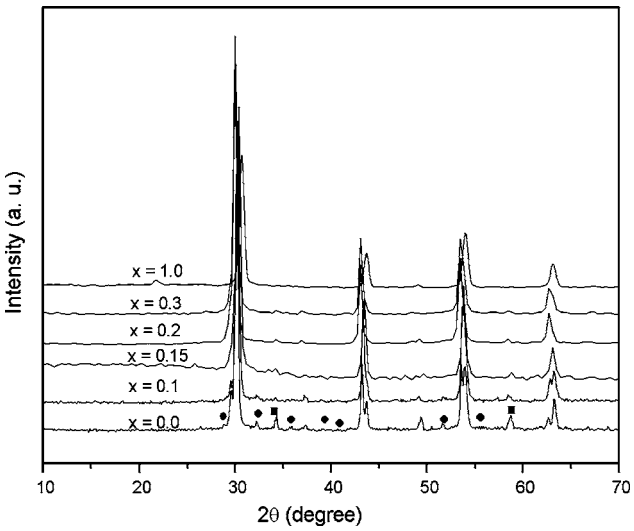

FIG. 1. X-ray diffraction pattern of $(Pb_{1-x}Ba_x)(Yb_{0.5}Ta_{0.5})O_3$ with $x=0.0$, 0.1, 0.15, 0.2, 0.3, and 1.0. The circles and squares represent the superlattice reflections due to antiparallel displacement of Pb and *B*-site ordering, respectively.

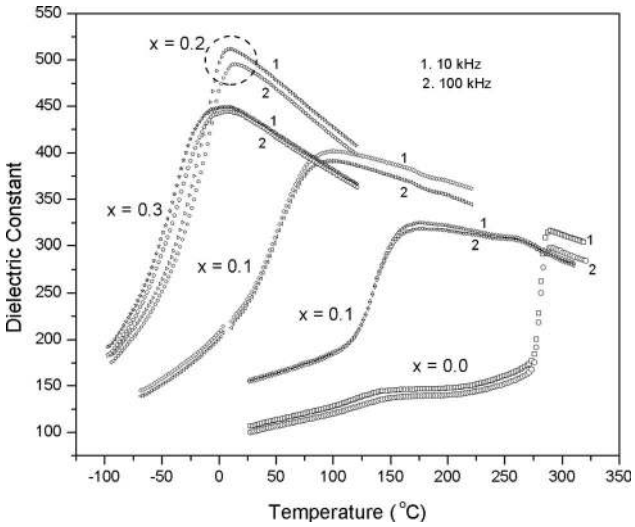

FIG. 2. The temperature variation of dielectric constant of $(Pb_{1-x}Ba_x)\times(Yb_{0.5}Ta_{0.5})O_3$, $x=0.0$, 0.1, 0.15, 0.2, and 0.3, at 10 and 100 kHz. The circle shows the dielectric dispersion observed at $x=0.2$.

state reaction method. Details of the sample preparation were discussed in our previous work except for the composition $x=1.0$.[7] Two-step solid-state reaction method was followed for the preparation of $Ba(Yb_{0.5}Ta_{0.5})O_3$ (BYT). The calcination and sintering temperatures were optimized to be 1325 °C for 4 h and 1600 °C for 4 h, respectively. The x-ray diffraction pattern of the samples was recorded at room temperature by Philips x-ray generator (PW140) using Cu $K\alpha(\lambda=1.5418)$ radiation in the 2θ range of 10°–70° at a scanning rate of 2° per minute. Low-frequency (0.1–200 kHz) dielectric measurements were carried out on the samples (except BYT) at the temperature range of −100–300 °C using Zentech 1061 *LCZ* meter. For Raman study, the sintered pellets were polished on one side using 0.25 μm diamond paste and subsequently annealed at 500 °C for 8 h to remove the residual surface stress left from polishing. The Raman scattering of the samples was carried out at room temperature in the frequency range of 20–1020 cm^{-1}. The spectra were recorded in back scattering geometry using 200 mW output power of 488 nm line of an Ar-ion laser. The scattered light was analyzed using a double monochromator (SPEX 14018) and detected with a photomultiplier tube (Hamamatsu R120) operating in a photon counting mode. The position, intensity, and full width at half maximum (FWHM) of the Raman peaks were obtained by fitting the spectra with Lorentzian line shape (Jandel PEAK FIT program).

III. RESULTS AND DISCUSSION

Figure 1 shows the x-ray diffraction patterns of $(Pb_{1-x}Ba_x)(Yb_{0.5}Ta_{0.5})O_3$, $x=0.0$, 0.1, 0.15, 0.2, 0.3, and 1.0. The circles and squares identify the superlattice reflection peaks due to Pb-antiparallel displacement and *B*-site ordering, respectively. The decrease in the intensity of the peaks indicates that the Pb-antiparallel displacement and *B*-site ordering start decreasing with increasing Ba concentration. However, some degree of ordering is retained even at $x=0.2$, as some weak peaks corresponding to *B*-site ordering are still seen in the x-ray diffraction pattern. The crystal structure changes to pseudocubic around $x=0.2$. The crystal structure of BYT is confirmed to be cubic after comparing with the Joint Committee on Power Diffraction (JCPDS) (CAS no.-19-0146) data. Thus, it indicates clearly that the increase in Ba concentration changes gradually the structure to cubic.

Figure 2 shows the temperature dependence of dielectric constant of $(Pb_{1-x}Ba_x)(Yb_{0.5}Ta_{0.5})O_3$, $x=0.0$, 0.1, 0.15, 0.2, and 0.3, at 10 and 100 kHz. The diffuseness in the dielectric constant curve increases with increase in Ba content. The dielectric constant curve for $x=0.2$ shows a weak dielectric dispersion (indicated by a circle in the dielectric curve) along with diffuseness and hence the composition behaves as a weak relaxor ferroelectric. The dielectric constant as well as diffuseness starts decreasing at $x=0.3$. This observation is expected because the end member of the series (BYT) is assumed to be a dielectric resonator as similar compounds such as $Ba(Yb_{0.5}Nb_{0.5})O_3$, $Ba(Y_{0.5}Ta_{0.5})O_3$, etc., are dielectric resonators. Generally the dielectric constant of these compounds is lower than that of lead-based compounds and it does not vary appreciably with temperature. Detailed analysis on dielectric properties of $(Pb_{1-x}Ba_x)(Yb_{0.5}Ta_{0.5})O_3$ is given elsewhere.[7]

The measured frequency range (20–1020 cm^{-1}) of the Raman spectra is split into three regions (20–200, 200–400, and 400–1020 cm^{-1}) and plotted in Figs. 3–5 for convenience. The overall spectra show that there is a broadening of certain peaks with substitution of Ba for Pb. This indicates some degree of disorder exits in the samples in comparison with the PYT sample, whereas the spectrum of BYT looks different from those of the lead-based compounds. The possible space group for PYT can be considered as $Fm\bar{3}m$ for the higher symmetry, cubic (paraelectric) and *Pbnm* for the lower-symmetry, orthorhombic (ferroelectric) phase.[4] We have assigned most of the intense peaks and performed a qualitative analysis of the changes observed upon Ba loading

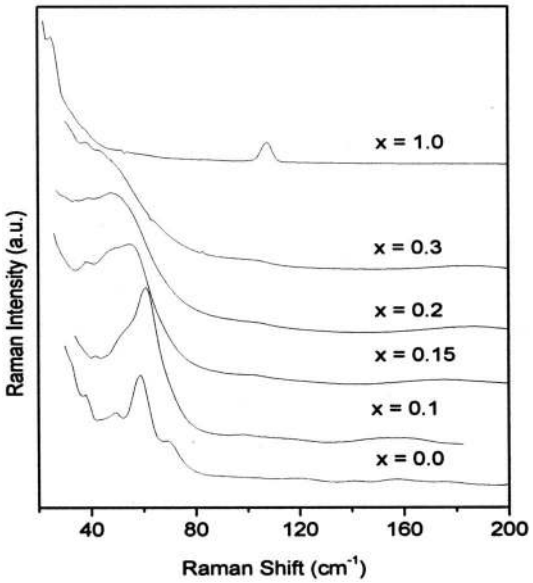

FIG. 3. Raman spectra of $(Pb_{1-x}Ba_x)(Yb_{0.5}Ta_{0.5})O_3$, x=0.0, 0.1, 0.15, 0.2, 0.3, and 1.0, in the frequency range of 20–200 cm^{-1}.

by following the available literature on similar systems of the same space group. The fitting parameters (the position and FWHM) of these modes are given in Table I. The factor group analysis for the cubic phase of the complex perovskites predicts vibrational modes corresponding to the following irreducible representations at the zone center:[13]

$$\Gamma = A_{1g} + E_g + 2F_{2g} + F_{1g} + 5F_{1u} + F_{2u}, \quad (1)$$

where one F_{1u} corresponds to a triply degenerate acoustical mode and the other four F_{1u} are infrared (IR) active optical modes. The F_{1g} and F_{2u} are the silent modes, which is neither IR nor Raman active. Finally, A_{1g},E_g, and $2F_{2g}$ are the four Raman-active modes.

The predicted 60 Raman-active modes for the orthorhombic phase are[14]

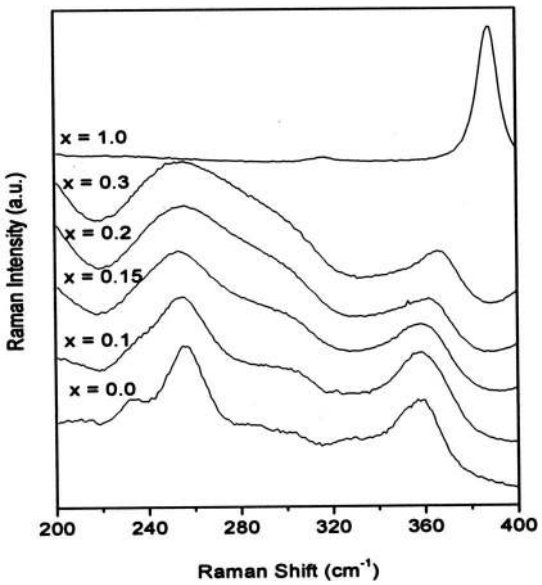

FIG. 4. Raman spectra of $(Pb_{1-x}Ba_x)(Yb_{0.5}Ta_{0.5})O_3$, x=0.0, 0.1, 0.15, 0.2, 0.3, and 1.0, in the frequency range of 200–400 cm^{-1}.

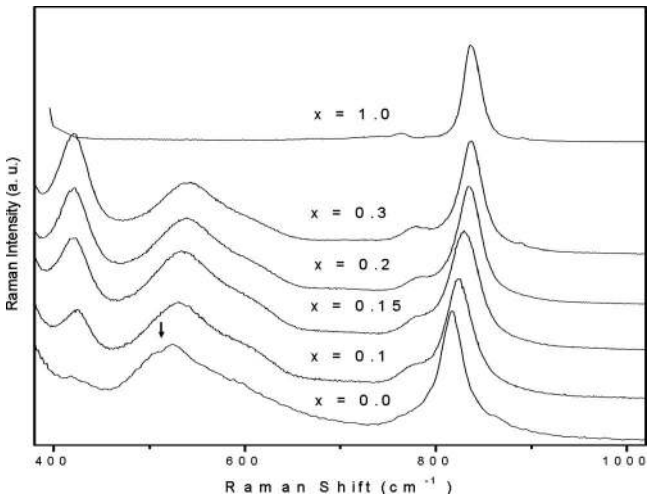

FIG. 5. Raman spectra of $(Pb_{1-x}Ba_x)(Yb_{0.5}Ta_{0.5})O_3$, x=0.0, 0.1, 0.15, 0.2, 0.3, and 1.0, in the frequency range of 400–1020 cm^{-1}.

$$\Gamma = 18A_g + 18B_{1g} + 12B_{2g} + 12B_{3g}. \quad (2)$$

The number of experimentally observed Raman peaks is less than 60. This may be due to merging of closely spaced modes due to thermal broadening, low polarizability, and degeneracy of certain modes. The number of modes observed for the compositions of cubic symmetry is more than the number predicted by group theory analysis. Thus, it gives evidence that there is a deviation of the local structure from the average, global structure. Therefore for our system, it is difficult to assign the symmetry of the modes solely on the basis of group theoretical analysis. Hence, we have followed the work of Mihailova *et al.* on PSN and PST system[15] for the lead-based compounds and Gregora *et al.* on ordered $Ba(Y_{0.5}Ta_{0.5})O_3$ system[16] for BYT to assign the modes.

It is well known for complex perovskites that for A_{1g} and E_g modes, the oxygen atoms are moving along the B'–O–B'' axis and all the cations are at rest. Hence there is no cationic mass effect on the modes and the corresponding frequencies are primarily determined by the B'–O and B''–O binding forces. However, for F_{2g} mode, the A cations are allowed to move along with the oxygen atoms. So the corresponding frequencies are expected to be influenced by the mass of A ion and the A–O binding energy. During the A_{1g} symmetry vibration, the movement of oxygen atoms along B'–O–B'' generates a strong peak at a relatively high frequency.[15,17] Thus the A_{1g} mode is assigned to the intense peak that appears consistently in all the Raman spectra at 820 cm^{-1}. It can be observed from Table I that the FWHM of the A_{1g} mode increases up to the composition around x=0.2. Similarly the intensity of this mode increases up to the composition around x=0.2 that can be observed in Fig. 5. According to the dielectric data the relaxor behavior increases up to the composition around x=0.2 and then starts decreasing (Fig. 2). Thus the changes observed in A_{1g} mode may be due to the decrease in degree of ordering as evident from x-ray analysis and the results agree well with the dielectric data. Similar tendency has been observed by Jiang *et al.*[18,19] for La^{3+} substituted lead magnesium niobate (PMN) system, as the narrowing of the A_{1g} mode has been attributed to increase in the

TABLE I. Raman peak positions (ω) and linewidth (Γ) in cm^{-1}.

	F_{2g}				F_{1u}				F_{1g}		F_{2u}				E_g		A_{1g}	
x	ω	Γ	ω	Γ	ω	Γ	ω	Γ	ω	Γ	ω	Γ	ω	Γ	ω	Γ	ω	Γ
0.0	59	4	527	27	256	12	⋯	⋯	209	11	303	9	357	11	⋯	⋯	817	12
0.1	58	8	530	51	255	18	425	19	207	16	297	30	357	13	775	13	824	17
0.15	57	9	534	49	253	23	422	21	199	15	294	37	358	18	780	21	830	18
0.2	56	12	538	46	254	29	421	20	201	9	292	29	362	9	784	28	835	15
0.3	46	16	540	43	266	27	421	19	200	8	297	22	367	9	782	30	837	14
1.0	⋯	⋯	⋯	⋯	254	9	⋯	⋯	⋯	⋯	315	5	⋯	⋯	763	14	838	9

B-site ordering. The shift of A_{1g} peak towards the higher frequency is essentially related to the variation of the B''–O distance and it occurs due to the movement of oxygen atom along B'–O–B'' which modifies the size of the *A* cation as the *B* cations are at rest.

The mode at 776 cm^{-1} is assigned to the E_g mode related to the stretching of $B''O_6$ octahedra. For PYT, the mode is not seen (may have merged with A_{1g} mode), but it starts appearing with increasing Ba concentration and is prominent for BYT. The mode shifts towards higher frequency up to 784 cm^{-1} and further shifts back to lower frequency for higher concentration of Ba. Similar variation is also observed in FWHM of the mode.

The two modes observed at 520 and 59 cm^{-1} are assigned to F_{2g} symmetric bending of BO_6 octahedra and Pb-localized mode, respectively. The F_{2g} modes are triply degenerate in cubic symmetry but split into three lines as the symmetry reduces to orthorhombic.[14] The splitting observed for the mode near 520 cm^{-1} for pure PYT sample (marked by an arrow in Fig. 5) vanishes. It is also seen that the splitting of the peak at 59 cm^{-1} reduces with the increase in Ba concentration. Similar observations are found in XRD pattern; the splitting of some fundamental peaks disappeared with Ba concentration as the symmetry of sample changes to cubic. It is expected that the frequency of the lower-energy F_{2g} mode should increase in Ba content, as the mass of Ba is less than Pb. With increase in Ba content, the frequency of this mode decreases to 46 cm^{-1} and FWHM increases to 16 cm^{-1} as can be seen in Table I. This indicates considerable softening of the force constant of the corresponding vibration. The broadening observed with increase in Ba may be due to the disordered distribution of Ba ions.

The modes at 255 and 420 cm^{-1} are assigned to the asymmetric O–*B*–O bending vibration having F_{1u} symmetry arising from rhombohedral structural distortion.[20] It is seen that the 420 cm^{-1} mode is absent in the spectra of PYT and appears at $x=0.1$. The intensity of the mode increases up to $x=0.2$ then starts decreasing at $x=0.3$ and vanishes for BYT. This observation is expected for higher concentration of Ba as the mode is also found to be absent in the spectra of a similar system $Ba(Y_{0.5}Ta_{0.5})O_3$.[16] Further the group theoretical analysis predicts only four Raman-active modes for a cubic $Fm\bar{3}m$ symmetry. However, more number of modes are observed in the Raman spectra for the composition $x=0.2$ and 0.3. This may be due to the existence of additional lower symmetry structure in the system. In a similar system $Pb_{1-x}Ba_x(Yb_{0.5}Nb_{0.5})O_3$, the evolution of hysteresis loop and gradual disappearance of heat capacity anomaly is attributed to the appearance of local polar regions of low symmetry within nonpolar matrix.[21] Based on detailed x-ray and neutron diffraction studies, de Mathan *et al.* reported the existence of 1:1 *B*-site nanopolar clusters and local rhombohedral $R3m$ symmetry, in addition to the average cubic symmetry for $Pb(Mg_{1/3}Nb_{2/3})O_3$ system.[22] Similarly, it has been reported that the presence of mode at 420 cm^{-1} in the Raman spectra of Sr substituted $LaMnO_3$ is due to the existence of orthorhombic phase with rhombohedral distortion.[23,24] Recently, Vedantam *et al.*.[25] also suggested that the existence of 420 cm^{-1} mode might be due to rhombohedral distortion and reported as one of the possible factors for the increase in diffuseness with substitution of Ba for Pb in $Pb(Yb_{0.5}Nb_{0.5})O_3$ (PYN) system. They observed the appearance of rhombohedral distortion from $x=0.05$ (which was absent for PYN) even though the dielectric response began to show diffuseness at $x=0.1$, since the Raman spectra probe the structural variation within a few unit cells. It is observed that PYN exhibits almost similar variation in structural and dielectric properties as observed in PYT with substitution of Ba. However, the variation observed for the mode at 420 cm^{-1} is rather gradual in Ba substituted PYT than that of Ba substituted PYN as a function of composition. Comparing the x-ray data of both the systems, it is observed that the PYT system exhibits higher degree of disorder than that of PYN with substitution of Ba. Hence, for the present case, the occurrence of more number of modes in the Pb-based compounds than in BYT and the appearance of the mode at 420 cm^{-1} may also be attributed to the existence of local rhombohedral distortion. The increase in intensity of the mode further suggests that the degree of distortion increases with Ba content. Correspondingly, the dielectric response becomes more diffused and exhibits relaxor behavior.

The two Raman peaks at 303 and 353 cm^{-1} arise from the F_{2u} modes due to electron-phonon coupling of Pb^{2+} lone pair electrons.[26,27] The FWHM of these two modes increases with increase in Ba concentration up to $x\approx 0.2$ then starts decreasing at $x>0.2$ and finally almost vanishes for BYT. The F_{2u} mode consists of O vibrations along the Pb–O bonds, i.e., it appears as a Pb–O bond-stretching mode in lead-oxygen system. This mode becomes Raman active under the lack of center of inversion, which occurs from off-centered displacement of Pb^{2+} ions. The Pb^{2+} cations can easily form elongated lone pairs if they are linked with *B*

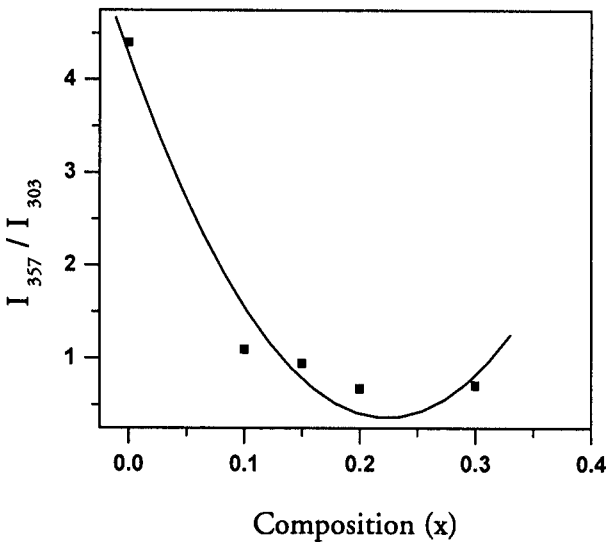

FIG. 6. The variation of the ratio I_{357}/I_{303} with chemical composition.

cations of different valence. The atoms may shift from ideal positions due to difference in covalency of the B'–O and B''–O bonds and in such a manner lone pairs oriented along the direction of the shift in the B cations appear. The shift in the position of Pb^{2+} ions, and the orientation of lone pair electrons depend on the local symmetry.[28] The XRD patterns (Fig. 1) indicate that the intensity of reflection peaks corresponding to antiparallel off-centered displacement of Pb^{2+} ions decreases gradually with increase in Ba^{2+} concentration. According to earlier reports,[15,28] if B-site ordering exists, the orientations of lone pairs are correlated and all Pb^{2+} atoms shift in the same direction with respect to O atoms. If the B-site ordering does not exist then there is random shift in Pb^{2+} and hence the electron lone pair orientations. Thus, the ratio of intensities of the peaks I_{357}/I_{303} is a measure of the chemical ordering at B site. The higher the ratio the more is the ordering and vice versa. The ratio decreases as the Ba concentration increases (Fig. 6). The decrease in the chemical ordering is also observed in the broadening of the A_{1g} phonon mode. Therefore, the decrease in the intensity ratio (I_{357}/I_{303}) of the peaks is attributed to the decrease in the chemical ordering in B site. The presence of ions of different valence and ionic size in the B site results in the relative rotation of octahedron due to size mismatch in B'–O–B'' bond. This gives rise to F_{1g} mode near 200 cm^{-1}. The mode shifts towards lower frequency but no regular trend has been observed in variation of intensity and FWHM.

It can be inferred from the above discussions that the phonon modes at 55, 520, 772, and 812 cm^{-1}, corresponding to the F_{2g}, E_g, and A_{1g} symmetry vibrations, are true Raman-active modes for the space group $Fm\bar{3}m$. The presence of $F_{2g}(55\ cm^{-1})$ and $A_{1g}(812\ cm^{-1})$ modes in all the spectra indicates the doubling of the unit cell, as both the end member compositions are highly ordered systems. The electron-phonon coupling due to Pb^{2+} lone pair electrons leads to modes at 303 and 353 cm^{-1} and the intensity ratio of the two peaks gives an idea about the change in ordering with composition. The gradual broadening observed in A_{1g} mode and the decrease in the intensity ratio (I_{357}/I_{303}) indicate the decrease of B-site order, which is in accordance with the x-ray diffraction and dielectric studies. Some of the extra modes (140,157, and 198 cm^{-1}) present due to orthorhombic symmetry disappear gradually with increase of Ba concentration as it is seen in XRD that the crystal structure changes to cubic at the composition around $x=0.2$. The presence of modes at 200, 255, and 420 cm^{-1} indicates the existence of lower symmetry structure, which is attributed to the local rhombohedral distortion. The variation in the Raman data follows a similar trend as in the case of x-ray diffraction and dielectric data with the substitution of Ba. Raman data suggest that the distortion is absent in end composition. However, in between compositions, the distortion increases up to $x=0.2$ and then decreases. Similarly, it has been observed in the x-ray diffraction and dielectric data that the degree of disorder increases up to $x=0.2$ and then starts decreasing with increase in Ba concentration. Therefore, it can be inferred that nanopolar clusters are formed even at low concentration of Ba, develop up to certain concentration ($x=0.2$), and then start disappearing for higher concentration of Ba.

IV. CONCLUSION

Raman scattering of $(Pb_{1-x}Ba_x)(Yb_{0.5}Ta_{0.5})O_3, x=0.0$, 0.1, 0.15, 0.2, 0.3, and 1.0, has qualitatively been studied in combination with x-ray diffraction and dielectric measurements. Raman spectra show a good agreement with the possible conclusions drawn from x-ray diffraction and dielectric spectroscopic experiments. Some of the peaks observed in the Raman spectra of pure PYT disappear upon Ba loading, which is related to the decrease in intensity of superlattice reflections due to Pb-antiparallel displacement. Thus, there is a clear indication of emergence of ferroelectric phase in the samples, as observed in the dielectric data. The increase of FWHM for A_{1g} mode and the decrease in the ratio I_{357}/I_{303} indicate a higher degree of disorder in the mixed samples as compared to the end member compositions. The diffuseness in the dielectric data may be due to the decrease in the degree of order with substitution of Ba in A site and to the presence of lower local symmetry, assigned to the rhombohedral distortion as revealed by Raman spectra.

[1] L. E. Cross, Ferroelectrics **76**, 241 (1987)
[2] M. E. Lines and M. A. Glass, *Principles and Applications of Ferroelectrics and Related Materials* (Oxford, New York, (1977).
[3] N. Yasuda and J. Konda, Appl. Phys. Lett. **62**, 535 (1993).
[4] P. Sciau, N. Lampis, and A. G. Lehmann, Solid State Commun. **116**, 225 (2000).
[5] Y. Park and K. M. Knowels, Jpn. J. Appl. Phys., Part 1 **37**, 3386 (1998).
[6] H. Kim, T. H. Hwang, J. H. Kim, and W. K. Choo, J. Eur. Ceram. Soc. **24**, 1501 (2004).
[7] D. Rout, V. Subramanian, K. Hariharan, V. Sivasubramanian, and V. R. K. Murthy, Ferroelectrics **300**, 67 (2004).
[8] *Handbook of Raman Spectroscopy: From the Research Laboratory to the process line*, edited by I. R. Lewiss and H. G. M. Edward (Marcel Dekker Inc., New York, 2001).
[9] N. Setter and I. Laulicht, Appl. Spectrosc. **41**, 526 (1987).
[10] I. G. Siny, R. Tao, R. S. Katiyar, R. Guo, and A. S. Bhalla, J. Phys. Chem. Solids **59**, 181 (1998).
[11] H. Ohwa, M. Iwata, H Orihara, N. Yasuda, and Y. Ishibashi, J. Phys. Soc. Jpn. **70**, 3149 (2001).
[12] E. Husson, L. Abello, and A. Morell, Mater. Res. Bull. **25**, 539 (1990).
[13] U. Bismayer, V. Devarajan, and P. Groves, J. Phys.: Condens. Matter **1**,

6977 (1989).
[14]G. Baldinozzi, P. Sciau, and A. Bulou, J. Phys.: Condens. Matter **7**, 8109 (1995).
[15]B. Mihailova, U. Bismayer, B. Guttler, M. Gospodinov, and L. Konstantinov, J. Phys.: Condens. Matter **14**, 1091 (2002).
[16]I. Gregora, J. Petzelt, J. Pokorny, V. Vorlicek, and Z. Zikmund, Solid State Commun. **94**, 899 (1995).
[17]M. L. Duyckaerts and P. Tarte, Spectrochim. Acta, Part A **30A**, 1771 (1974).
[18]F. Jiang, S. Kojima, C. Zhao, and C. Feng, J. Appl. Phys. **88**, 3608 (2000).
[19]F. Jiang, S. Kojima, C. Zhao, and C. Feng, Appl. Phys. Lett. **79**, 3938 (2001).
[20]A. Kania, E. Jahfel, G. E. Kugel, K. Roleder, and M. Hafid, J. Phys.: Condens. Matter **8**, 4441 (1996).
[21]W. K. Choo and H. Y. Kim, J. Phys.: Condens. Matter **4**, 2309 (1992).
[22]N. de Mathan, E. Husson, G. Calvarn, J. R. Gavarri, A. W. Hewat, and A. Morell, J. Phys.: Condens. Matter **3**, 8159 (1991).
[23]E. Granado *et al.*, Phys. Rev. B **58**, 11435 (1998).
[24]P. Bjornsson, M. Rubhausen, J. Backstrom, M. Kall, S. Eriksson, J. Eriksen, and L. Borjesson, Phys. Rev. B **61**, 1193 (2000).
[25]R. R. Vedantam, V. Subramanian, V. Sivasubramanian, and V. R. K. Murthy, J. Phys.: Condens. Matter **17**, 361 (2005).
[26]I. W. Chen, P. Li, and Y. Wang, J. Phys. Chem. Solids **57**, 1525 (1996).
[27]B. P. Burton, J. Phys. Chem. Solids **61**, 327 (2000).
[28]B. Guttler, B. Mihailova, R. Stosch, U. Bismayer, and M. Gospodinov, J. Mol. Struct. **661**, 469 (2003).